Article

Coupled and Decoupled Dual Quantum Systems in One Semiconductor Nanocrystal

David Battaglia, Bridgette Blackman, and Xiaogang Peng

J. Am. Chem. Soc., **2005**, 127 (31), 10889-10897• DOI: 10.1021/ja0437297 • Publication Date (Web): 19 July 2005

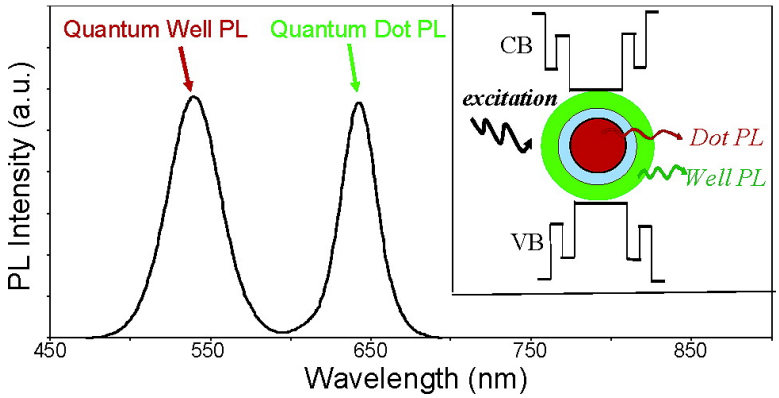

More About This Article

Additional resources and features associated with this article are available within the HTML version:

- Supporting Information
- Links to the 26 articles that cite this article, as of the time of this article download
- Access to high resolution figures
- Links to articles and content related to this article
- Copyright permission to reproduce figures and/or text from this article

View the Full Text HTML

J|A|C|S
ARTICLES
Published on Web 07/19/2005

Coupled and Decoupled Dual Quantum Systems in One Semiconductor Nanocrystal

David Battaglia, Bridgette Blackman, and Xiaogang Peng*

Contribution from the Department of Chemistry and Biochemistry, University of Arkansas, Fayetteville, Arkansas 72701

Received October 14, 2004; E-mail: xpeng@uark.edu

Abstract: Dual quantum systems, 0-dimensional quantum dot, and 2-dimensional quantum wells were constructed in one II−VI semiconductor nanocrystal by the epitaxial growth of a barrier (ZnS) layer between the systems in solution. By alteration of the thickness of the barrier layer, the two quantum systems were controlled to either electronically coupled or decoupled. Evidence of optical coupling between the two band gap emissions was also observed. The position and relative intensity of the two emissions can be independently tuned by reaction conditions. Total photoluminescence quantum efficiency of the dual emitting bands reached as high as 30% at room temperature under synthetic conditions not optimized for high emission.

Introduction

Colloidal semiconductor nanocrystals are known as quantum dots,[1,2] rods,[3] and shells/wells,[4] each of which is a single quantum system on a single particle basis. Because of quantum confinement, the optical properties of colloidal semiconductor nanocrystals are strongly size or dimension dependent when their physical size is smaller than the diameter of the exciton of the given bulk semiconductor. Recent progress on the synthetic chemistry of semiconductor nanocrystals through organometallic approaches[5] and alternative approaches[6,7] has made it possible for the community to access high quality semiconductor nanocrystals with controlled size, shape,[3] optical properties,[8] and size/shape distribution. The advancement of the synthetic chemistry of colloidal nanocrystals has further promoted their technical applications in the field of light-emitting diodes (LEDs),[9,10] lasers,[11] solar cells,[12] biomedical labeling,[13,14] and gas sensing[15] as well as related fundamental studies, such as phase transition,[16] crystallization,[17] etc.

Band gap engineering—usually through molecular beam epitaxy and related UHV techniques—builds up artificial and complex band gap gradients in semiconductors by altering the chemical compositions, which yields semiconductors with unique electronic properties, such as quantum wells and superlattices.[18,19] Properties of colloidal semiconductor nanocrystals can be tuned by their physical size in the quantum confinement size regime.[1−4] If band gap engineering can be fully applied to nanocrystals, the resulting complex band gap structures will possess further means, in addition to quantum confinement, to manipulate their carriers (electrons and holes). Colloidal dual-emitting nanocrystals, in this report, reveal a great potential for such nanocrystals.

Synthesis of multiple quantum systems has been explored by several groups in the field of colloidal semiconductor nanocrystals because of the analogue mentioned in the above paragraph. The most noticeable attempts[20,21] were colloidal double-quantum wells based on the CdS−HgS system originally developed by Mews et al.[22] By use of a surface-replacement strategy, the authors tried to insert HgS layers between CdS barriers. The authors observed significant red-shift of the absorption spectra of the complex nanocrystals, indicating significant electric coupling between the two wells, although the absorption spectra were not sharp enough to judge the independence of each intended quantum system. Once activated in basic solutions, the complex nanocrystals usually showed a single band gap emission although it was broad and weak.

A new technique was introduced recently for the epitaxial growth of a colloidal compound semiconductor onto another,

(1) Brus, L. E. *J. Chem. Phys.* **1984**, *80*, 4403−9.
(2) Alivisatos, A. P. *Science* **1996**, *271*, 933−7.
(3) Peng, X.; Manna, U.; Yang, W.; Wickham, J.; Scher, E.; Kadavanich, A.; Allvisatos, A. P. *Nature (London)* **2000**, *404*, 59−61.
(4) Battaglia, D.; Li, J. J.; Wang, Y.; Peng, X. *Angew. Chem.* **2003**, *42*, 5035−5039.
(5) Murray, C. B.; Norris, D. J.; Bawendi, M. G. *J. Am. Chem. Soc.* **1993**, *115*, 8706−15.
(6) Peng, Z. A.; Peng, X. *J. Am. Chem. Soc.* **2001**, *123*, 183−184.
(7) Yu, W. W.; Peng, X. *Angew. Chem., Int. Ed.* **2002**, *41*, 2368−2371.
(8) Qu, L.; Peng, X. *J. Am. Chem. Soc.* **2002**, *124*, 2049−2055.
(9) Schlamp, M. C.; Peng, X.; Alivisatos, A. P. *J. Appl. Phys.* **1997**, *82*, 5837−5842.
(10) Mattoussi, H.; Radzilowski, L. H.; Dabbousi, B. O.; Thomas, E. L.; Bawendi, M. G.; Rubner, M. F. *J. Appl. Phys.* **1998**, *83*, 7965−7974.
(11) Klimov, V. I.; Schwarz, C. J.; McBranch, D. W.; Leatherdale, C. A.; Bawendi, M. G. *Phys. Rev. B: Condens. Matter* **1999**, *60*, R2177−R2180.
(12) Greenham, N. C.; Peng, X.; Alivisatos, A. P. *Phys. Rev. B: Condens. Matter* **1996**, *54*, 17628−17637.
(13) Bruchez, M., Jr.; Moronne, M.; Gin, P.; Weiss, S.; Alivisatos, A. P. *Science* **1998**, *281*, 2013−2016.
(14) Chan, W. C. W.; Nile, S. *Science* **1998**, *281*, 2016−2018.
(15) Nazzal, A. Y.; Qu, L.; Peng, X.; Xiao, M. *Nano Lett.* **2003**, *3*, 819−822.
(16) Alivisatos, A. P. *J. Phys. Chem.* **1996**, *100*, 13226−13239.
(17) Qu, L.; Yu, W. W.; Peng, X. *Nano Lett.* **2004**, *4*, 465−469.
(18) Herman, M. A.; Sitter, H. *Mol. Beam Epitaxy* **1996**.
(19) Nozik, A. J. *Annu. Rev. Phys. Chem.* **2001**, *52*, 193−231.
(20) Braun, M.; Burda, C.; El-Sayed, M. A. *J. Phys. Chem. A* **2001**, *105*, 5548−5551.
(21) Dorfs, D.; Eychmueller, A. *Nano Lett.* **2001**, *1*, 663−665.
(22) Mews, A.; Eychmueller, A.; Giersig, M.; Schooss, D.; Weller, H. *J. Phys. Chem.* **1994**, *98*, 934−41.

which is a modified version of successive ionic layer adsorption and reaction (SILAR).[23] Experimental results revealed this new SILAR technique can provide excellent control of the shell thickness with submonolayer accuracy for several semiconductor pairs.[4,23] This invited us to reconsider the growth of multiple quantum systems on a single nanocrystal, enabling sequential epitaxial growth of different semiconductor nanocrystals onto given core nanocrystals.

This report will concentrate on the formation of a zero-dimensional (0D) quantum system and a two-dimensional (2D) one in a single II−VI semiconductor nanocrystal (0D−2D nanocrystals). Experimental results reveal that the electronic and optical coupling between the two systems can be tuned by altering the ZnS barrier layer between the two quantum systems. In contrast to the strict requirement for the epitaxial growth on bulk substrates,[18,19] a procedure using the SILAR technique[4,23] with air-stable precursors successfully demonstrated the epitaxial growth of ZnS onto CdSe (13% lattice mismatch) up to five monolayers. Different from the conventional II−VI multiple quantum wells on bulk substrates,[24,25] the two independently tunable band gap emissions of 0D−2D nanocrystals were surprisingly strong at room temperature, up to 30% quantum yield. The new nanostructures may find applications for spintronics,[26] LEDs,[9,10] and molecular barcoding[27] and will also be unique for studying interactions between two quantum systems,[28] a challenging subject even for chemically coupled nanocrystal dimers.[29]

Experimental Section

Materials. Cadmium oxide (99.99%), zinc oxide (99.9%), selenium (99.5%, 100 mesh), sulfur (99.98%, powder), tributylphosphine (TBP, 97%), 1-octadecene (ODE), and oleic acid (OA 90%) were purchased from Aldrich. Octadecylamine (ODA, 98+%) was purchased from Lancaster. All organic solvents were purchased from EM Sciences. All chemicals were used directly without any further purification.

Synthesis of CdSe/ZnS/CdSe Dual Quantum Systems. All CdSe cores used were standard products of NN-Labs, which were prepared through the known alternate precursor methods for CdSe nanocrystal synthesis.[8,30] The Cd and Zn precursors (0.04M) were made by dissolving CdO/ZnO in OA (1:8 molar ratio) and ODE under Ar. The mixture was then sealed and heated at 240 °C until the solution turned clear. The Se precursor (0.04M) was made by dissolving pure Se powder in tributylphoshine (TBP) (1:16 molar ratio) and ODE under Ar. The S precursor (0.04M) was made by adding pure S in ODE and heating at 100 °C under Ar until it is dissolved.

For a typical reaction, CdSe core nanocrystals of a known size and concentration, typically 1.25×10^{-8} mol for this research, were added to a reaction flask with 3.0 g of ODA and 3.0 g of ODE. The reaction was put under vacuum and heated to 100 °C. The reaction was then flooded with Ar and steadily added as the reaction is further heated to 200 °C. For growth of the ZnS layers, the Zn precursor was added first followed by the S precursor 5 min later. The Zn and S were allowed to react for up to 30 min before another layer of ZnS was applied. Between 1 and 5 monolayers of ZnS were grown for this study. For the growth of the CdSe or CdS outer layers, the heat was decreased to 190 °C from 200 °C, and the Cd and Se (or S) precursors were added in the same manner as for the ZnS layers. Enough precursor was added for growth of only one monolayer at a time, which was calculated using the previous method.[23] One monolayer of ZnS, CdS, and CdSe was approximated to be a 0.7 nm increase in diameter/size as estimated previously.[23] The actual sizes of the resulting nanocrystals were measured using a transmission electron microscope (see details below), and, furthermore, consistent with the expected values within experimental error. Both the ZnS and CdSe (or CdS) were layered on in the same process in a one-pot reaction. After the final layers of CdSe (CdS) were added, the reaction was heated to 240 °C for up to 30 min. Next, the reaction was allowed to cool to 70 °C, then hexanes was added, followed by an excess of methanol, to enable a known purification process through extraction.[31] This created two layers, a nonpolar (hexanes/ODE with nanocrystals) layer and a methanol layer. The nonpolar layer was kept, and the nanocrystals were precipitated out with further excess amounts of acetone followed by centrifugation. The resulting nanocrystals were dispersible in nonpolar solvents such as hexanes, toluene, and choloroform.

Optical Measurements. Absorption spectra were measured on a HP 8453 diode array spectrophotometer. Photoluminescence (PL) and photoluminescence excitation (PLE) were measured on a Spex Fluorolog 3-111 using a PMT detector. PL quantum yields (QY) of the samples were determined through comparison using organic dyes with known quantum yields as standards.[8] All samples for measurement consisted of nanocrystals dissolved in ~1 mL of solvent. The excitation wavelength was set at 400 nm, except the ones with CdS as the outer shell (350 nm excitation being used in these cases).

Transmission Electron Microscopy (TEM). The low-resolution transmission electron microscopy images were taken on a JEOL 100CX transmission electron microscope with an acceleration voltage of 100 kV. High-resolution TEM was performed on a Philips CM200 operating at 200 kV. All of the samples were purified through the known extraction method using hexanes and methanol. Formvar film-coated copper grids were dipped in diluted toluene solutions to deposit the nanocrystals onto the film. Concentrations of the nanocrystal solutions used for dipping were controlled by keeping the absorbance of the first absorption peak below 0.2. Selected-area electron diffraction (SAED) patterns were taken with a camera length of 120 cm.

Etching Experiments. The surface ligands of the nanocrystals were exchanged from ODA to benzylamine. The rigid and short tail of benzylamine, in comparison to the long and flexible hydrocarbon chain of ODA, made the etching process efficient. For example, benzylamine-coated CdSe nanocrystals were obtained by placing 0.5 mL of ODA-coated CdSe nanocrystals of a known size and concentration in about 2 mL of benzylamine, which was then sonicated for approximately 10 min, or until the nanocrystals were totally dispersed yielding a clear solution. Subsequently, the sonicated nanocrystal solution (0.1 mL) was added to 0.5 mL of a 3:1 toluene/methanol solution. To initiate the etching process, each of these solutions was mixed with 100 μL of a 0.165 M benzoyl peroxide solution (1:1 toluene/methanol solvent). The etching process was monitored using an Ocean Optics USB2000 UV−visible spectrometer, which provided absorption measurements in real time with an adequate time resolution.

Results and Discussions

The barrier layer between two adjacent quantum systems must structurally allow epitaxial growth between different semiconductors and electronically control quantum mixing of the quantum systems. In conventional band gap engineering on single-crystalline substrates, the allowed lattice mismatch is very

(23) Li, J. J.; Wang, Y. A.; Guo, W.; Keay, J. C.; Mishima, T. D.; Johnson, M. B.; Peng, X. *J. Am. Chem. Soc.* **2003**, *125*, 12567−12575.
(24) Cibert, J.; Gobil, Y.; Dang, L. S.; Tatarenko, S.; Feuillet, G.; Jouneau, P. H.; Saminadayar, K. *Appl. Phys. Lett.* **1990**, *56*, 292−4.
(25) Zajicek, H.; Juza, P.; Abramof, E.; Pankratov, O.; Sitter, H.; Helm, M.; Brunthaler, G.; Faschinger, W.; Lischka, K. *Appl. Phys. Lett.* **1993**, *62*, 717−19.
(26) Awschalom, D. D.; Flatte, M. E.; Samarth, N. *Sci. Am.* **2002**, *286*, 67−73.
(27) Han, M.; Gao, X.; Su, J. Z.; Nie, S. *Nat. Biotechnol.* **2001**, *19*, 631−635.
(28) Ouyang, M.; Awschalom, D. D. *Science* **2003**, *301*, 1074−1078.
(29) Peng, X.; Wilson, T. E.; Alivisatos, A. P.; Schultz, P. G. *Angew. Chem., Int. Ed. Engl.* **1997**, *36*, 145−147.
(30) Qu, L.; Peng, Z. A.; Peng, X. *Nano Lett.* **2001**, *1*, 333−337.
(31) Yu, W. W.; Qu, L.; Guo, W.; Peng, X. *Chem. Mater.* **2003**, *15*, 2854−2860.

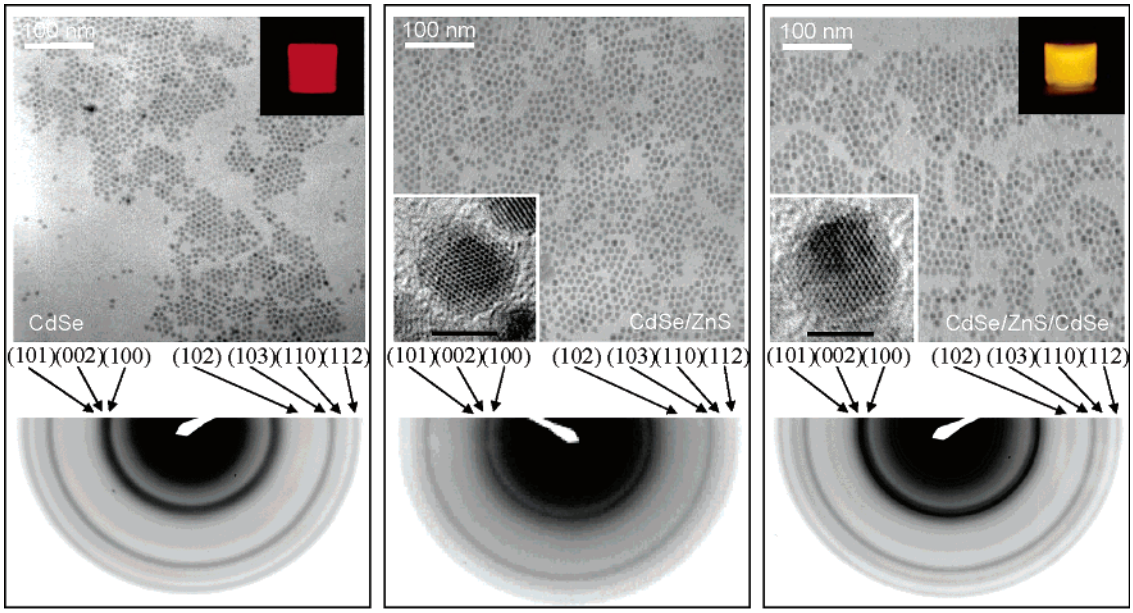

Figure 1. TEM and SAED of the nanocrystals for (left) CdSe (the core), (middle) CdSe/ZnS with 3 monolayers of ZnS, and (right) CdSe/ZnS/CdSe with 3 outer layers of CdSe. High-resolution TEM is provided for the CdSe/ZnS (inset) and CdSe/ZnS/CdSe (inset) samples to further show crystal structure (the scale bar for HRTEM is 5 nm). The emission pictures of the CdSe cores (inset) and CdSe/ZnS/CdSe (inset) are also shown.

small even for relatively more tolerant II−VI semiconductors. For example, of the CdSe multiple quantum wells, ZnSe was chosen as the barrier layer (about 5% lattice mismatch).[25] Because the bulk band gap difference between ZnSe (about 2.7 eV) and CdSe (about 1.75 eV) is small, a ZnSe layer thicker than 100 nm was needed to sufficiently decouple the two CdSe quantum systems.[25] Multiple band gap emission from such built CdSe multiple quantum wells was only observed under low temperatures. It is impractical to epitaxially grow a barrier with a thickness more than 100 nm for colloidal nanocrystals. Even if this could be done, the resulting particles will significantly vary the optical properties of the colloidal solution, due to their light scattering properties.

In this work, CdSe—bulk band gap equal to 1.75 eV—was chosen as the 0D and 2D quantum system because of the well-developed synthesis and relatively well-studied optical properties of the 0D and 2D quantum systems. CdS (bulk band gap 2.5 eV) and ZnSe with thicknesses over 10 monolayers were confirmed by us to be insufficient barriers for isolating the 0D and 2D systems. Strong coupling between HgS wells through a CdS barrier was also observed in the case of CdS/HgS/CdS/HgS/CdS colloidal multiple quantum wells.[20,21] As reported previously, a significant red-shift of the absorption and PL spectra of the CdSe/CdS core/shell nanocrystals was observed, indicating the substantial delocalization of the electron and hole wave functions into the shell semiconductor.[23,32,33] It is well known that a ZnS (bulk band gap 3.7 eV) shell can efficiently confine the excitons generated in CdSe nanocrystals.[33,34] However, the large lattice mismatch (about 13%) between ZnS and CdSe made the epitaxial and controllable growth of ZnS onto CdSe with substantial thickness quite difficult using the traditional organometallic approach, indicated by the appearance of a set of separated diffraction rings of ZnS lattice, in addition, to the original ones of CdSe lattice.[33]

The great flexibility provided by SILAR coupled with air-stable and generic precursors[23] was used for optimizing the epitaxial growth of ZnS layers on CdSe nanocrystals up to five monolayers. As shown in Figure 1, only one set of diffraction rings for wurtzite structure in SAED was observed in all different growth stages. We found that the growth temperature, the concentration of amines added into the growth solution, and the chain length of the fatty acids for zinc and cadmium precursors were all important factors for this interesting success. The growth temperature could not be very high because it might cause Ostwald ripening of the core or core/shell nanocrystals. However, too low of a growth temperature caused insufficient growth of the ZnS shell, which is similar to that observed for the growth of CdS shells onto CdSe core nanocrystals.[23] The optimal temperature range under the tested conditions was identified to be around 200−240 °C. At this temperature, a relatively high amine concentration was found necessary to activate the zinc fatty acid salts (the greener precursors).[35] Typically, we observed that the initial ratio between primary amine and ODE needed to be near 50%. However, too much primary amines in the reaction solution would make it difficult to purify and characterize the resulting nanocrystals because of the crystalline feature of the primary amines at room temperature. Observed previously, ODE, as the noncoordinating solvent, provided a desired processibility of the final product because of its liquid nature at room temperature.

High-resolution TEM images of the complex nanocrystals, shown as insets in Figure 1, further confirmed the single crystalline feature of the CdSe/ZnS and CdSe/ZnS/CdSe nanocrystals. The successful epitaxial growth of the CdSe−ZnS system, in this report, supports the hypothesis[36] that the tolerance of the lattice mismatch significantly increases as the dimension

(32) Peng, X.; Schlamp, M. C.; Kadavanich, A. V.; Alivisatos, A. P. *J. Am. Chem. Soc.* **1997**, *119*, 7019−7029.
(33) Dabbousi, B. O.; Rodriguez-Viejo, J.; Mikulec, F. V.; Heine, J. R.; Mattoussi, H.; Ober, R.; Jensen, K. F.; Bawendi, M. G. *J. Phys. Chem. B* **1997**, *101*, 9463−9475.
(34) Hines, M. A.; Guyot-Sionnest, P. *J. Phys. Chem.* **1996**, *100*, 468−71.
(35) Li, L. P. N.; Wang, Y.; Peng, X. *Nano Lett.* **2004**, in press.
(36) Yang, P. *Heterogeneous Silicon−Germanium Nanowires*; Boston, 2002.

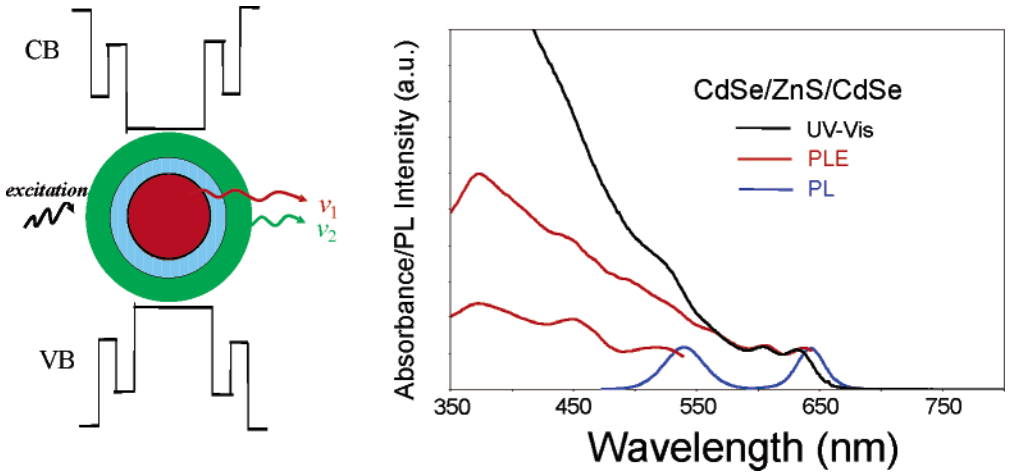

Figure 2. (left) A diagram demonstrating the band structure and emission of the sample when excited. (right) UV−vis, PL (PL excitation at 400 nm), and PLE is shown for the CdSe/ZnS/CdSe sample.

of the materials decreases from 3D (bulk crystals) to 1D (nanowires and nanorods)[37] and, further, to 0D (spherical nanocrystals) in this case. It should be pointed out that, in the literature of MBE, II−VI semiconductor systems have been observed to be more tolerant in terms of lattice mismatch than III−V systems.[24,25] This may also contribute to the success of the current system. In principle, the structural data supported the epitaxial growth between CdSe and ZnS, because the lattice mismatch between CdSe and ZnS should still cause substantial strain between these two materials. Therefore, the influence of this strain on the properties of the CdSe/ZnS core/shell nanocrystals and CdSe/ZnS/CdSe core/shell/shell nanocrystals are worth researching in careful studies. Significantly, more systematic experimental data will be needed for a possible theoretical model.

Figure 2 displays the spectroscopic properties of the 0D−2D nanocrystals. The PL spectrum shows two distinguished peaks, both of which are sharp and similar to those observed for typical 0D and 2D systems. The PLE spectra (red lines in Figure 2) of the two PL peaks indicate that the low-energy PL peak is associated with the core (0D) and the high-energy one possesses the features of typical 2D systems.[4] The PLE of the low-energy PL peak followed the absorption spectrum of the sample nicely at the low-energy part and showed significantly low intensity at the high-energy portion where the absorption of the 2D quantum system resided. The total PL QY of the two band gap emissions was observed as high as about 30%, although the growth conditions were not optimized for achieving highest PL QY at present. The absorption spectrum is a sum of the two quantum systems (comparing the absorption and PLE spectra in Figure 2). The PL color of the 0D−2D nanocrystals is white-yellow (inset in Figure 1, top right), which is significantly different from the original red color of the core CdSe nanocrystals (inset in Figure 1, top left).

The peak positions of both PL peaks of the 0D−2D nanocrystals can be independently tuned. The position of the band gap PL peak of the 0D quantum system can be altered by choosing different sized cores to start with (Figure 3, left). By use of the same core, the band gap PL of the 2D quantum shells was shifted to red by changing the thickness of the shell (from top to bottom in Figure 3, middle). By use of a different quantum shell material, such as CdS together with a barrier of 4 monolayers of ZnS, the emission peak position of the 2D emission can be extended to the optical windows, which CdSe 2D systems cannot cover (Figure 3, top right).

Furthermore, the relative intensities of the two PL bands were variable by annealing the nanocrystals for different amounts of time (Figure 3 bottom right). Since the 2D system is on the outer surface of the 0D−2D nanocrystals, annealing significantly increased its PL intensity without significantly varying the intensity of the core emission. Although the exact mechanism for this enhancement is unknown, it is likely a result of better surface ligand coverage, as observed previously. Enhanced solubility in nonpolar solvents of the 0D−2D nanocrystals obtained by annealing, also supports the fact that the intensity increase of the 2D PL was due to the improvement of the ligand passivation on the surface of the nanocrystals. It was reported previously that the surface structure/reconstruction of nanocrystals might be improved by annealing 0D CdSe nanocrystals when amines were presented as the ligands.[38]

Evidently, the variation of the relative intensity of the two PL bands dramatically changed the PL color of the 0D−2D nanocrystals (inset, Figure 3, right bottom), varying from pink (no annealing), to pale yellow (short annealing), to bright green (long annealing time). It should be pointed out that the relative intensity of the two PL bands remained stable, if the annealing stopped at a certain time and the resulting nanocrystals were stored at room temperature.

The two quantum systems in the 0D−2D-hybridized nanocrystal can be electronically coupled. The degree of interaction depends on the thickness of the ZnS barrier layer. Figures 4 and 5 demonstrate that, with one monolayer of ZnS, no emission from the 2D system was observed. Furthermore, the PL peak of the 0D system (the core) shifted significantly to lower energy for the systems with one and two monolayers of ZnS and slightly to the blue for thick ZnS barrier layers (three and four monolayers). The colloidal double quantum well systems (CdS−HgS−CdS−HgS−CdS), reported previously, showed a red-shift of the overall absorption and PL spectra, but it was difficult to distinguish the contributions from the two wells.[20,21] The authors suggested that significant electronic coupling exists in their

(37) Wu, Y.; Fan, R.; Yang, P. *Nano Lett.* **2002**, *2*, 83−86.

(38) Talapin, D. V.; Rogach, A. L.; Kornowski, A.; Haase, M.; Weller, H. *Nano Lett.* **2001**, *1*, 207−211.

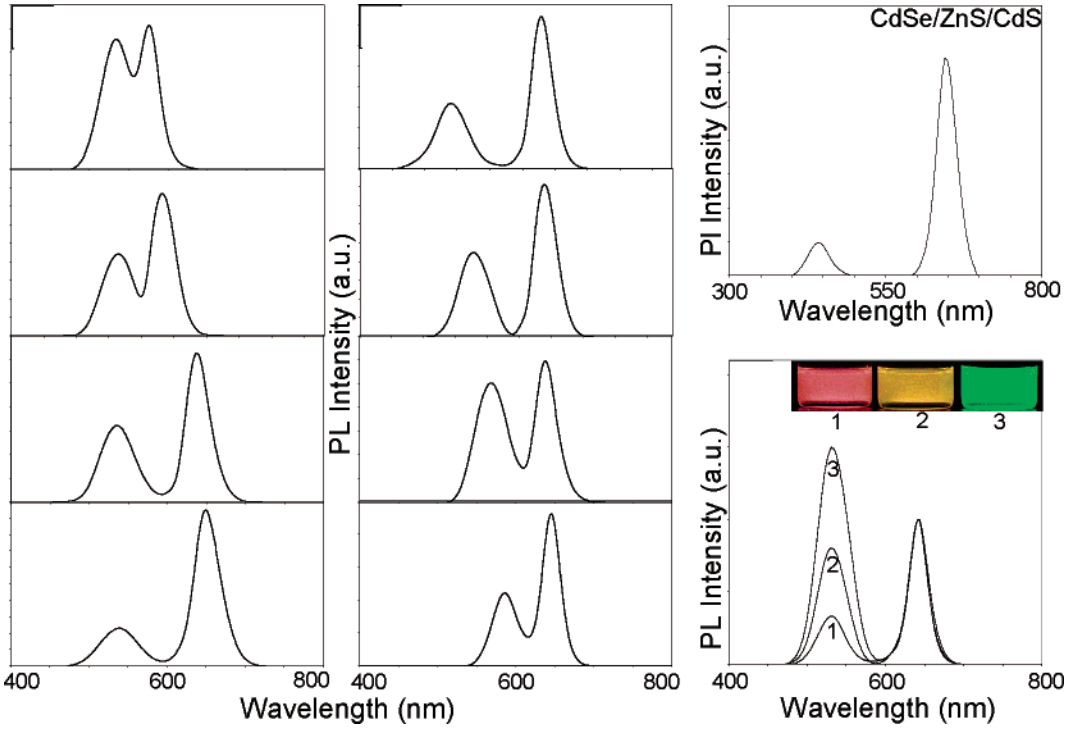

Figure 3. PL of CdSe/ZnS/CdSe nanocrystals excited at 400 nm with: (left) same CdSe shell thickness and different CdSe core sizes, 3.0, 3.5, 5.6, to 6.4 nm (top to bottom) and (middle) same CdSe core size with different CdSe shell thicknesses (1−4 monolayers). (top right) PL for a CdSe/ZnS/CdS sample (excitation at 350 nm). (bottom right) PL for a CdSe/ZnS/CdSe system showing the relative increase in the emission intensity of the CdSe shell as well as the variation of the emission color as the CdSe/ZnS/CdSe nanocrystals were annealed at 240 °C. Annealing times: (1) original sample, (2) 15 min, (3) 30 min.

systems.[20,21] With two monolayers of ZnS as the barrier layer, a relatively weak PL peak from the 2D system was observed and some red shift of the 0D PL was evident. Three to four monolayers of ZnS were typically thick enough to significantly isolate the two-emission systems. As a result, the PL peak of the original 0D system did not show significant shift upon the further growth of the CdSe 2D system, and a relatively strong PL peak for the 2D system was observed. A slight blue shift, more or less within experimental error, upon the growth of the first monolayer of CdSe for the hybridized nanocrystals with three or four monolayers of ZnS spacing layer was observed (Figures 4 and 5). At this moment, the cause of the blue shift is still under investigation.

For CdSe/ZnS/CdSe 0D−2D nanocrystals, if the thickness of the ZnS layer was five monolayers or more, the epitaxial growth of the subsequent CdSe quantum shells became difficult under the growth conditions examined.

Figure 4 (bottom right) quantitatively illustrates the perturbation for the 0D quantum system by the growth of the 2D system, indicated by the red-shift of the PL peak of the 0D quantum system against the thickness of the quantum shells. The 0D−2D nanocrystals with one or two monolayers of ZnS barrier layers (Figure 4, top) are somewhat similar to superlattices in conventional semiconductor sciences, in which the two-quantum systems strongly interact with each other. The decoupled ones (three or four monolayers of ZnS barrier layer) are similar to the multiple quantum wells. It should be pointed out that controlled electronic coupling between two semiconductor nanocrystals in nanocrystal dimers has not been achieved, although nanocrystal dimers were fabricated previously.[29] Furthermore, synthesis of colloidal semiconductor nanocrystal dimers with controlled interparticle distances is significantly more complicated than that for the formation of 0D−2D nanocrystals shown here.

With any number of ZnS monolayers, no 2D PL was detected if the thickness of the CdSe quantum shell was only one monolayer, which is similar to the isolated quantum shells grown directly on nanocrystal templates with a wide band gap.[4] However, the growth of a single monolayer of CdSe onto the CdSe/ZnS nanocrystals did affect the PL peak position of the 0D system for a thin ZnS barrier layer (Figure 5) and strongly enhanced the PL intensity of the 0D system for all tested ZnS thicknesses. The reasons for this enhancement are not clear at present, although it may be due to a better match between the ligands (amines) and the surface composition (CdSe instead of ZnS).[4]

When the PL of the 0D system (the core) was at higher energy than the absorption onset of the 2D system (well), the PL of the core of the 0D−2D nanocrystals became undetectable (Figure 6). This may partially be due to the reabsorption of the PL of the core by the quantum shell which completely surrounded the core (see detail below). The unique spatial and electronic configurations of the two quantum systems should also improve the efficiency of Forster energy transfer from the core to the outer shell quantum well, in comparison to the reversed energy transfer (see below). Figure 4 showed that the PL intensity of the quantum shells were relatively weak when only two monolayers of ZnS existed in comparison to the relatively thick ZnS barriers. This result is consistent with the existence of Forster energy transfer, which strongly depends on the distance between two quantum systems involved,[39]

(39) Achermann, M.; Petruska, M. A.; Kos, S.; Smith, D. L.; Koleske, D. D.; Klimov, V. I. *Nature (London)* **2004**, *429*, 642−646.

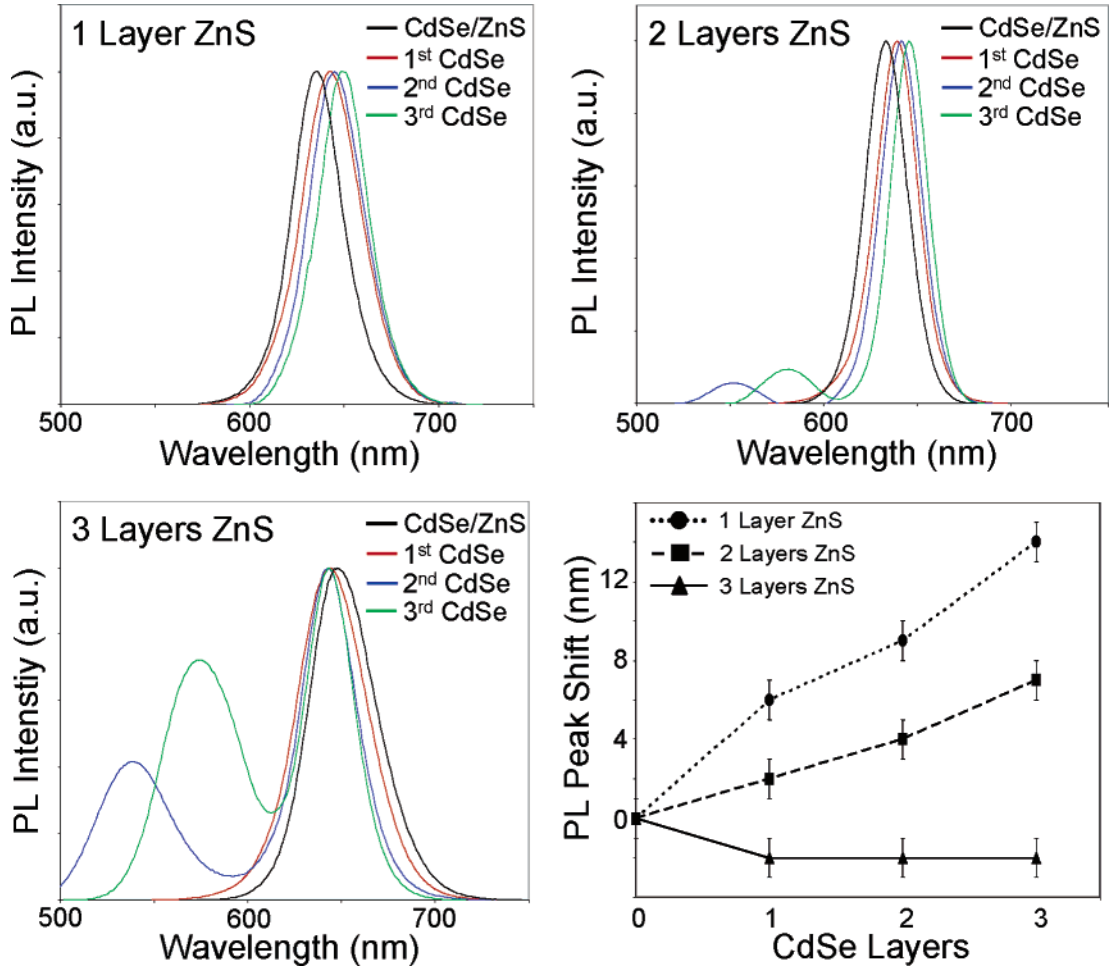

Figure 4. PL spectra of CdSe/ZnS/CdSe nanocrystals by varying the ZnS barrier layer, 1 ZnS layer (top left), 2 ZnS layers (top right), and 3 ZnS layers (bottom left). (bottom right) A quantitative comparison of the CdSe core emission peak shift as the CdSe shell is layered on for the CdSe/ZnS/CdSe samples having different ZnS barrier thicknesses.

although electronic coupling may also lead to similar results (see discussion above).

When two quantum systems are close to each other, within a few nanometers, Forster energy transfer should be present. The PL property difference between the two different cases in Figure 6, single PL band vs two PL bands, indicates that the configuration between the acceptor quantum system and the donor quantum system in the 0D−2D nanocrystals is playing a key role. In literature, it has been demonstrated that the energy transfer either between nanocrystal and dye molecules[40] or between nanocrystals[41] strongly depends on the number of nearest acceptors presented around the donor nanocrystal. In other words, the distance and the configuration of donor/acceptor both play critical roles in determining the efficiency of energy transfer. For the 0D−2D nanocrystals with a thin CdSe shell in Figure 6, the core CdSe was the acceptor and the donor was the shell. This relationship switched when the CdSe shell layer had grown to five monolayers for the system shown in Figure 6.

Klimov's group proposed that the efficiency of Forster energy transfer between nanocrystals within nanocrystal solid films should be proportional to the number of nearest acceptors surrounding each donor nanocrystal. Perhaps a case which is more close to the system discussed here is the nanocrystal-dye energy transfer system studied by Medintz et al.[40] They found that the quenching efficiency of the PL of a given nanocrystal strongly depended on the number of dye acceptors attached to the nanocrystal, increased from about 25 to 60% as the dye acceptor increased from one per nanocrystal to about 5 per nanocrystal. For a comparison, the current system could be approximated to the two schematic drawings shown in Figure 7.

When the shell was the donor (thin shell case, top panel, Figure 7), the acceptor in the same particle, the core, was located only in one direction of the exciton. However, in this situation, both the oscillator strength of the acceptor (see below) and configuration was changed substantially as the core became the donor when the shell thickness passed a certain level (Figure 7, bottom). Instead of a single acceptor, the donor was surrounded with a continuous layer of acceptors, which is approximated as a dense layer of spherical acceptors in Figure 7. Within approximately the same radius around the exciton, in both cases in Figure 7, there is only one acceptor available at a relatively small solid angle when the dot is the acceptor, (top, Figure 7) and there is a full monolayer of acceptors when the quantum shell is acting as the acceptor (bottom, Figure 7). In the pictures in Figure 7, the wave function of the exciton was

(40) Medintz, I. L.; Trammell, S. A.; Mattoussi, H.; Mauro, J. M. *J. Am. Chem. Soc.* **2004**, *126*, 30−31.
(41) Achermann, M.; Petruska, M. A.; Crooker, S. A.; Klimov, V. I. *J. Phys. Chem. B* **2003**, *107*, 13782−13787.

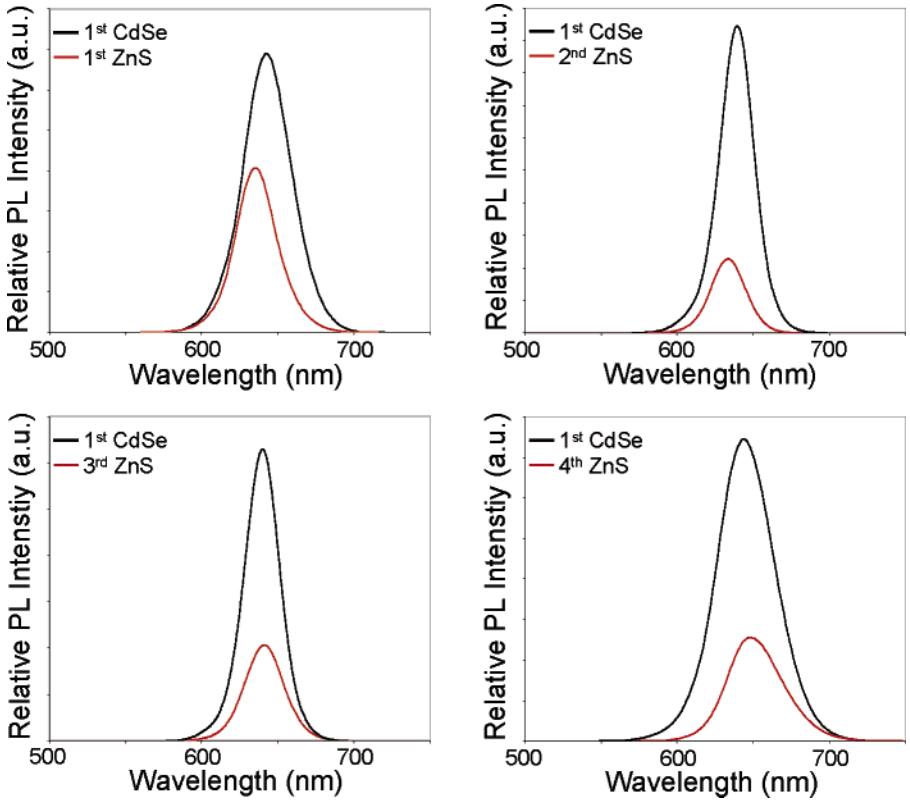

Figure 5. PL spectra of CdSe/ZnS with different ZnS thickness (1−4 monolayers) along with the PL spectra after 1 monolayer of CdSe was grown. (top left) 1 ZnS layer, (top right) 2 ZnS layers, (bottom left) 3 ZnS layers, (bottom right) 4 ZnS layers.

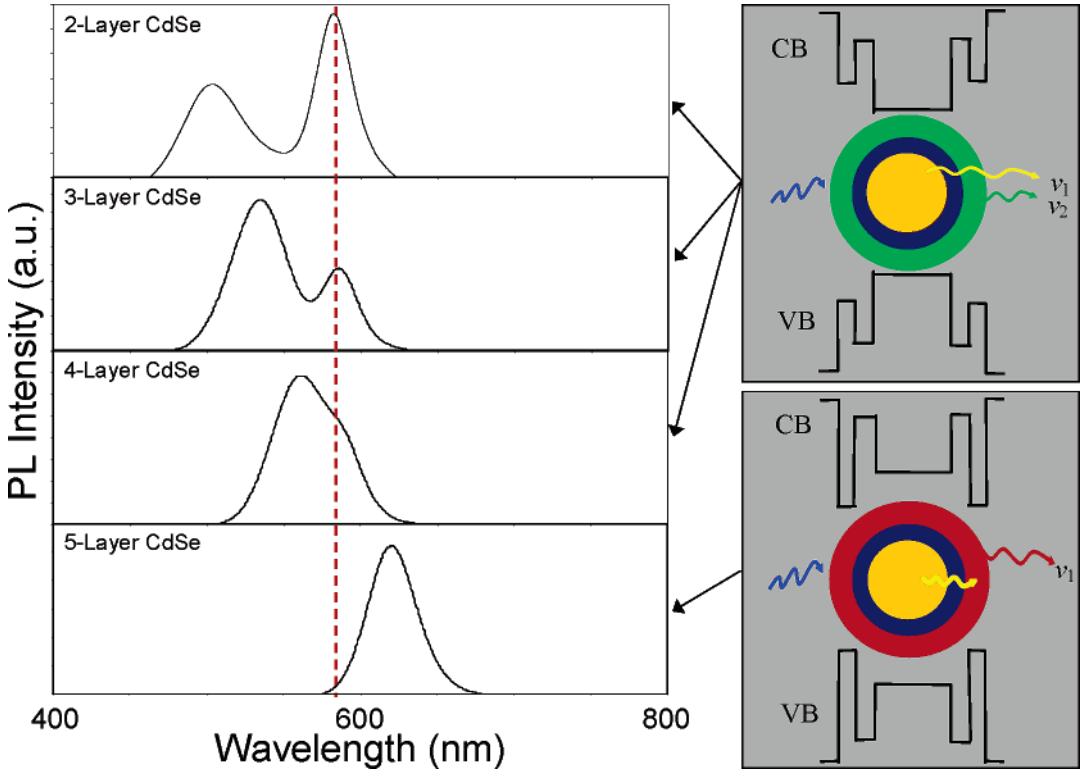

Figure 6. (left) Optical coupling of the CdSe/ZnS/CdSe samples by varying the CdSe shell thickness (absorption onset) until the PL (absorption onset) of the shell is shifted to higher wavelength than that of the CdSe core. (right) Band diagrams demonstrating the band structure within the nanocrystals as the CdSe shell thickness (band gap) is increased (decreased).

considered to have a spherical symmetry or a spherical distribution of the transition dipole in the time frame of interest. Therefore, a significantly more efficient energy transfer should be expected as observed in the literature.[40]

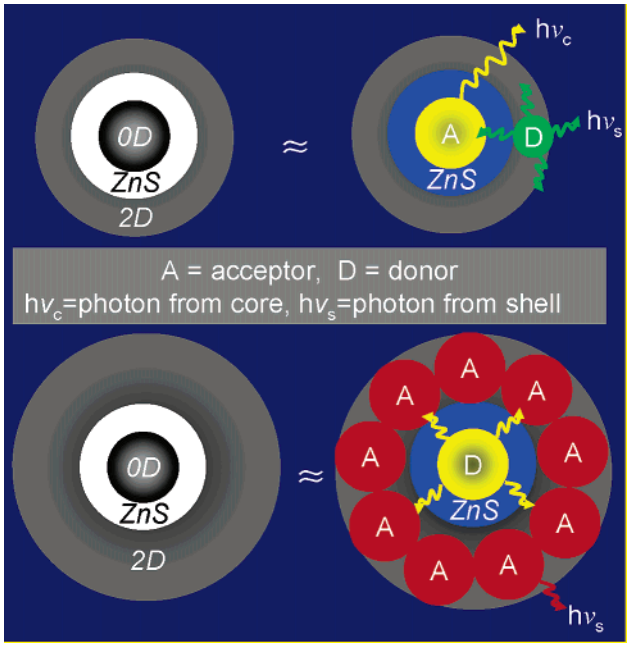

Figure 7. Schematic illustration of energy transfer between 0D and 2D quantum systems in a single nanocrystal with two different configurations. Dual-emission bands should be detected for the top system and a single PL band should result from the bottom case.

Even though Figure 7 was based on the information for Forster energy transfer, it should also be a reasonable representation for energy transfer through reabsorption, if an emission wave generated by an exciton recombination in both the quantum shell and dot can be approximated as a spherical wave.

It is interesting to compare the volume of the acceptors for the two different cases shown in Figures 6 and 7 since extinction coefficients—or total oscillator strength—of both quantum dots and wells per particle/well are dependent on their volume.[4] For both, Forster energy transfer and reabsorption, the efficiency increases as the total oscillator strength of the acceptor increases, if the spectral overlap is approximately the same.

For the system shown in Figure 6, the total volume of the core dot as a sphere and the CdSe quantum shell as a ring can be approximately estimated by eqs 1 and 2, respectively.

$$V_{\text{dot}} = 4/3\pi r^3_{\text{dot}} \quad (1)$$

$$V_{\text{shell}} = 4/3\pi r^3_{\text{shell}} - 4/3\pi r^3_{\text{CdSe/ZnS}} \quad (2)$$

Here, V_{dot} and V_{shell} are the volume of the dot acceptor (top cases in Figure 6) and quantum shell acceptor (bottom one in Figure 6), respectively. The radii of the dot, final 0D−2D structures, and CdSe/ZnS coated nanocrystals are respectively represented as r^3_{dot}, r^3_{shell}, and $r^3_{\text{CdSe/ZnS}}$, which were about 1.7, 3.1 (core plus four monolayers of ZnS), and 4.9 (core plus four monolayers of ZnS and five monolayers of CdSe) sequentially for the system in Figure 6. The volume ratio of the shell acceptor and the dot acceptor will thus be

$$V_{\text{shell}}/V_{\text{dot}} = (r^3_{\text{shell}} - r^3_{\text{CdSe/ZnS}})/r^3_{\text{dot}} \approx 18 \quad (3)$$

This result implies that the picture in Figure 7 (bottom), approximating a quantum shell acceptor as a continuous monolayer of acceptors, is semiquantitatively correct. Both total oscillator strength and configuration likely contributed to the different optical coupling in Figure 6. The schematic picture in Figure 7 further implies that energy transfer from an outer quantum shell to an inner quantum well should be more efficient than that from a quantum shell to a quantum dot. This is because an inner quantum well quencher has a larger volume and a bigger solid quenching angle, in comparison to an inner quantum dot quencher with the same absorption edge and the same distance to an exciton at the most outer quantum shell. This hypothesis is actually consistent to our preliminary results. All efforts intended to build dual emission nanocrystals based on dual quantum wells have not been successful up to this point.

The optical data discussed above are consistent with the core/shell/shell structures proposed for the 0D−2D quantum systems. This structure can be further verified by optical measurements performed during controlled etching experiments to be discussed below.

It was previously observed that peroxide can controllably etch CdSe nanocrystals under certain conditions.[31] Brock's group recently reported that peroxides can etch CdSe much more efficiently than CdS.[42] We applied this etching strategy to CdSe, CdSe/ZnS core/shells, and CdSe/ZnS/CdSe 0D−2D systems (Figure 8).

Within the same time frame, CdSe core nanocrystals were almost completely etched, indicated by the rapid blue-shift and decrease of the absorbance (Figure 8, left). CdSe/ZnS core/shell nanocrystals (with three monolayers of ZnS), however, behaved differently from the core nanocrystals under the same etching conditions (Figure 8, middle panel). The absorption showed a slight blue-shift (about 2−3 nm) initially, and further changes of the absorption spectrum were not visible under the time scale shown (tens of seconds). It took about a day to reach the same final stage as the plain core nanocrystals (Figure 8, left). This indicates a well-protected CdSe core nanocrystal. Interestingly, Alivisatos's group reported recently that small molecules can diffuse through a polycrystalline shell, even though the shell appeared to be dense under the two-dimensional project image of high-resolution TEM.[43] Therefore, the results (Figure 8, middle panel) are consistent with a dense ZnS shell on the surface of CdSe core nanocrystals.

The CdSe/ZnS/CdSe 0D−2D nanocrystals (Figure 8, right panel) were etched in a different pattern, in comparison to the plain core and CdSe/ZnS core/shell nanocrystals. A rapid decrease of the absorbance at the high energy side in the absorption—with the low energy peaks pretty much untouched—was evidenced. After the spectrum resembled the original CdSe/ZnS core/shell nanocrystals, the etching process stopped. These observations are consistent with the proposed structure of the 0D−2D systems, with the unprotected quantum shell on the surface and protected (by ZnS middle shell) quantum dot as the core. As discussed above, (See Figure 2 and related discussions about absorption and PLE spectra), quantum shells only contribute to the absorption at the high-energy side.

The dual-emitting nanocrystals with controlled intensities and peak positions have significant advantages for molecular barcoding using nanocrystals because of the ease of loading into the polymer beads.[27] In addition to this potential application, these nanocrystals may also be of importance for LEDs[9,33] with

(42) Mohanan, J. L.; Arachchige, I. U.; Brock, S. L. *Science* **2005**, *307*, 397−400.
(43) Yin, Y.; Rioux, R. M.; Erdonmez, C. K.; Hughes, S.; Somorjai, G. A.; Alivisatos, A. P. *Science* **2004**, *304*, 711−714.

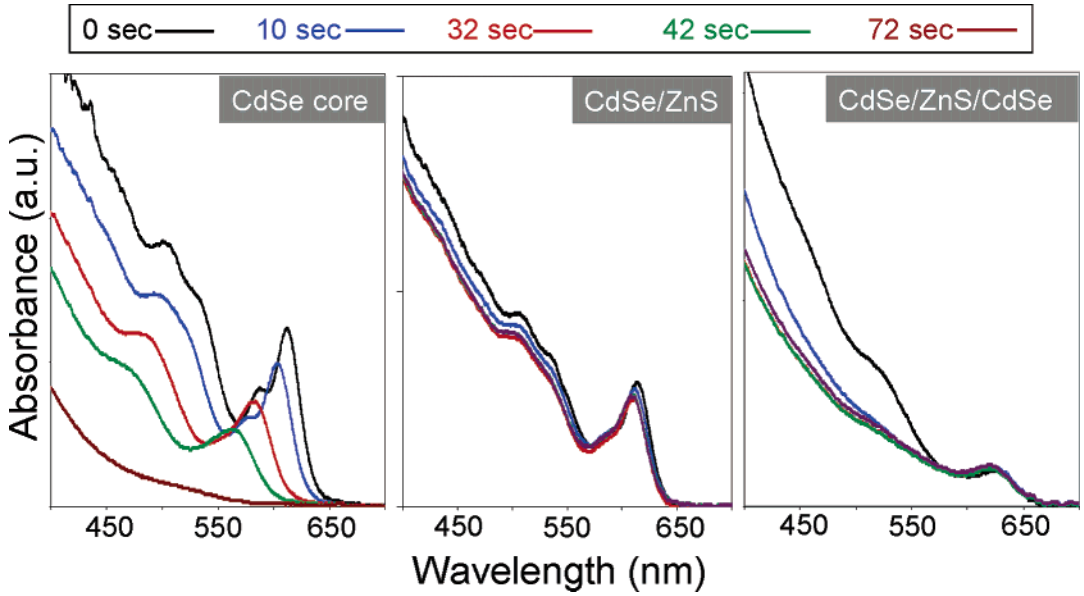

Figure 8. Etching of nanocrystals with different structures using benzyl peroxide. The etching time is given at the top.

specific emission profiles. Position and intensity tunable emitters with multiple emission bands may also provide some new opportunities for biomedical labeling using colloidal semiconductor nanocrystals. The 0D−2D-hybridized nanocrystals reported here are also unique for studying coupling between different quantum systems. At present, electronic and optical coupling between quantum systems related to colloidal semiconductor nanocrystals has been limited to ensemble cases.[28] The nanocrystals described in this report may make it possible for studying such interactions at a single molecular level because of the relatively bright PL and defined structure.

Conclusion

In summary, using ZnS as the barrier layer, CdSe 0D and 2D quantum systems can be built as electronically coupled or decoupled by varying the ZnS barrier layer thickness from one to four monolayers. The spatial configuration, composition, and synthetic chemistry of the 0D−2D nanocrystals are not much more complicated, in comparison to known core/shell and quantum well nanocrystals.[4,22,23,34,44−46] However, the realization of the dual-emitting 0D−2D nanocrystals indicate that band gap engineering, which has played a critical role in conventional semiconductor sciences, may foster many new quantum structures for the field of colloidal nanocrystals. This should shed new light on existing technical applications of semiconductor nanocrystals, ranging from LEDs,[9,10] biomedical labeling,[13,14] to molecular barcoding.[27] These new nanocrystals may also open a door for new applications using nanocrystals, such as energy convention,[12] catalysis,[47] spintronics,[26] etc. The spatial and electronic arrangements of 0D−2D and other potential dual/multiple quantum systems are also interesting and unique samples for studying the quantum couplings of semiconductor nanocrystals.[28]

Acknowledgment. Financial support from the NSF is acknowledged. We also appreciate the high-resolution TEM work done by David R. Hull and Dr. Stephanie Castro of the NASA Glenn Research Center.

JA0437297

(44) Kim, S.; Fisher, B.; Eisler, H.-J.; Bawendi, M. *J. Am. Chem. Soc.* **2003**, *125*, 11466−11467.
(45) Cao, Y.; Banin, U. *J. Am. Chem. Soc.* **2000**, *122*, 9692−9702.
(46) Manna, L.; Scher, E. C.; Li, L.-S.; Alivisatos, A. P. *J. Am. Chem. Soc.* **2002**, *124*, 7136−7145.
(47) Kraeutler, B.; Bard, A. J. *J. Am. Chem. Soc.* **1978**, *100*, 4317−18.